

ℓ_1 -Norm Minimization with Regula Falsi Type Root Finding Methods

Metin Vural, Aleksandr Y. Aravkin, and Sławomir Stańczak

Abstract—Sparse level-set formulations allow practitioners to find the minimum 1-norm solution subject to likelihood constraints. Prior art requires this constraint to be convex. In this letter, we develop an efficient approach for nonconvex likelihoods, using Regula Falsi root-finding techniques to solve the level-set formulation. Regula Falsi methods are simple, derivative-free, and efficient, and the approach provably extends level-set methods to the broader class of nonconvex inverse problems. Practical performance is illustrated using ℓ_1 -regularized Student’s t inversion, which is a nonconvex approach used to develop outlier-robust formulations.

Index Terms— ℓ_1 -norm minimization, nonconvex models, Regula-Falsi, root-finding

I. INTRODUCTION

SPARSE recovery using ℓ_1 -norm minimization plays a major role in many signal processing applications. Denoting $\mathbf{y} \in \mathbb{R}^M$ as a measurement vector, $\mathbf{D} \in \mathbb{R}^{M \times N}$ as an overcomplete matrix with $M < N$, and ρ as the penalty that measures the data misfit, the ‘noise-aware’ level-set problem is to minimize ℓ_1 -norm subject to a misfit or likelihood constraint:

$$(P_\sigma) \quad \underset{\mathbf{x} \in \mathbb{R}^N}{\text{minimize}} \quad \|\mathbf{x}\|_1 \quad \text{s.t.} \quad \rho(\mathbf{y} - \mathbf{D}\mathbf{x}) \leq \sigma,$$

where σ indicates the noise level. P_σ is used in many applications, including compressed sensing [1] [2], overcomplete signal representation [3], [4], coding theory [5], and image processing [6].

An efficient way to solve (P_σ) is to develop an explicit relationship with a simpler problem that can be directly solved with primal-only methods, such as the prox-gradient algorithm [7]:

$$(P_\tau) \quad \underset{\mathbf{x} \in \mathbb{R}^N}{\text{minimize}} \quad \rho(\mathbf{y} - \mathbf{D}\mathbf{x}) \quad \text{s.t.} \quad \|\mathbf{x}\|_1 \leq \tau.$$

Exploiting the relationship between P_σ and P_τ allows one to specify the noise tolerance σ , and then find the solution by inexactly optimizing a sequence of simpler (P_τ) problems.

It has been known for a long time that (P_τ) and (P_σ) can provide equivalent solutions [8], and the idea of solving (P_τ) to obtain the solution of (P_σ) was first proposed by [9], [10]. Their idea follows the optimality trade-off between the minimum ℓ_1 -norm and the least squares data misfit, which generates a differentiable convex Pareto frontier. This optimality tracing is formulated as a non-linear equation root finding problem, i.e. getting the exact τ for a given noise tolerance σ , and is solved by an inexact Newton Method. The resulting level-set approach has been generalized to other instances of convex programming by [7], [11].

In the most general case, the relationship between (P_τ) and (P_σ) does not require convexity [11, Theorem 2.1]. However, practical implementations of the root-finding approach require convexity of the Pareto frontier to guarantee success of the root finding procedure, limiting the approach to the convex case. Current implementations favor Newton’s method, which requires derivatives. To address this issue, an extension using an inexact secant method has also been developed [7].

In this paper, we introduce *Regula Falsi* type derivative-free non-linear equation root finding schemes to solve (P_σ) . They are bracketing type methods that offer convergence guarantee for convex and nonconvex models with the proper choices of root searching interval: two initial points with the opposite signs assures convergence [12]. *Regula Falsi* type methods do not require convexity to trace the root, allowing nonconvex loss functions in the (P_σ) formulations. Finally, these methods are also derivative free. All of these advantages allow *Regula Falsi* type methods to be applied to cases where Newton, secant, and their variants are not guaranteed to converge.

Moving outside of the convex class opens the way for using many useful nonconvex models in (P_σ) formulations. For example, in [13] and [14] consider mixture models whose negative log-likelihood are nonconvex, with applications to high-dimensional inhomogeneous data where number of covariates could be larger than sample size. A second application area uses nonconvex Student’s t likelihoods to develop outlier-robust approaches [15]–[17]. In this paper, we show how *Regula Falsi* type root finding methods can be used with the nonconvex Student’s t loss, as well the convex least-squares and Huber losses.

This paper is organized as follows. In Section II, a Pareto frontier that reveals the relation between (P_τ) and (P_σ) is defined and *Regula Falsi* type methods are introduced. Section III presents the proposed (P_σ) solver while the simulation results are discussed in Section IV.

II. PARETO FRONTIER AND REGULA FALSI-TYPE ROOT FINDING METHODS

Under simple ‘active constraint’ conditions, problems (P_τ) and (P_σ) are equivalent for some pair (τ, σ) [11]. Pareto frontier approaches use root finding and inexact solutions to a sequence of (P_τ) to solve (P_σ) .

A. Pareto Optimality

Definition 1: i) *Pareto optimal* is the minimal achievable feasible point of a feasible set. ii) The set that comprised of Pareto optimal points is called the *Pareto frontier*.

In this work, we also seek to solve (P_σ) by working with (P_τ) . Specifically, we are interested in the optimal objective

value of the (P_τ) for a given \mathbf{y} and τ which can be expressed with following

$$\nu(\tau) := \inf_{\mathbf{x}} \{\rho(\mathbf{D}\mathbf{x} - \mathbf{y}) \mid \|\mathbf{x}\|_1 \leq \tau\}, \quad (1)$$

and the corresponding *Pareto frontier* can be defined as

$$\psi(\tau) := \nu(\tau) - \sigma. \quad (2)$$

Theorem 1: i) If ρ is a convex function (e.g. ℓ_2 -norm, Huber function), then so is ψ . ii) If ρ is a nonconvex function, convexity of ψ does not follow. When ρ is quasi-convex function, then so is ψ .

Proof 1: Let us consider any two solutions \mathbf{x}_1 and \mathbf{x}_2 of (P_τ) for any τ_1 and τ_2 respectively. Since ℓ_1 -norm is convex, for any $\beta \in [0, 1]$ following holds

$$\begin{aligned} \|\beta\mathbf{x}_1 + (1 - \beta)\mathbf{x}_2\|_1 &\leq \beta\|\mathbf{x}_1\|_1 + (1 - \beta)\|\mathbf{x}_2\|_1 \\ &= \beta\tau_1 + (1 - \beta)\tau_2. \end{aligned} \quad (3)$$

An immediate outcome of eq. (3) is that $\beta\mathbf{x}_1 + (1 - \beta)\mathbf{x}_2$ is a feasible point of (P_τ) with $\tau = \beta\tau_1 + (1 - \beta)\tau_2$. Thus we can write the following inequality

$$\begin{aligned} \nu(\beta\tau_1 + (1 - \beta)\tau_2) &\leq \rho(\mathbf{D}(\beta\mathbf{x}_1 + (1 - \beta)\mathbf{x}_2) - \mathbf{y}) \\ &= \rho(\beta(\mathbf{D}\mathbf{x}_1 - \mathbf{y}) + (1 - \beta)(\mathbf{D}\mathbf{x}_2 - \mathbf{y})). \end{aligned} \quad (4)$$

i) If ρ is convex, then

$$\begin{aligned} \rho(\beta(\mathbf{D}\mathbf{x}_1 - \mathbf{y}) + (1 - \beta)(\mathbf{D}\mathbf{x}_2 - \mathbf{y})) &\leq \beta\rho(\mathbf{D}\mathbf{x}_1 - \mathbf{y}) + \\ &(1 - \beta)\rho(\mathbf{D}\mathbf{x}_2 - \mathbf{y}) = \beta\nu(\tau_1) + (1 - \beta)\nu(\tau_2), \end{aligned} \quad (5)$$

that shows ν is convex as well as ψ .

ii) If ρ is quasi-convex, then

$$\begin{aligned} \rho(\beta(\mathbf{D}\mathbf{x}_1 - \mathbf{y}) + (1 - \beta)(\mathbf{D}\mathbf{x}_2 - \mathbf{y})) &\leq \\ \max\{\rho(\mathbf{D}\mathbf{x}_1 - \mathbf{y}), \rho(\mathbf{D}\mathbf{x}_2 - \mathbf{y})\} &= \max\{\nu(\tau_1), \nu(\tau_2)\}, \end{aligned} \quad (6)$$

that shows ν is quasi-convex as well as ψ .

Pareto optimal points are unique for (P_τ) with convex and quasi-convex losses ρ that can be inferred from [18, Theorem 1.1, Theorem 1.2], [19]. Also, the feasible set of (P_τ) enlarges as τ increases, thus $\psi(\tau)$ is nonincreasing [20]. In Fig. 1 an abstract $\psi(\tau)$ is depicted for convex and quasi-convex losses ρ where the red line represents the σ level.

Obtaining the solution of (P_σ) by solving (P_τ) proceeds as follows. We start with a τ parameter to solve (P_τ) , and using the solution of (P_τ) , find a new τ value. We proceed iteratively until $\psi(\tau_\sigma) \rightarrow 0$. τ_σ occurs at the intersection of the red line and black curve in Fig 1, where we immediately see that the solution of (P_τ) is also a solution of the (P_σ) , a fact proven formally by [11]. Finding τ_σ can be formulated as a nonlinear root finding problem.

B. Regula Falsi Type Methods

Our aim is to

$$\text{find } \tau \text{ such that } \psi(\tau) = 0. \quad (7)$$

If ρ is nonconvex, neither Newton's method nor secant variants are guaranteed to solve (7). In particular, the tangent lines may cross in the feasible region, and secant lines may not bracket the feasible area. In contrast, regardless of shape of

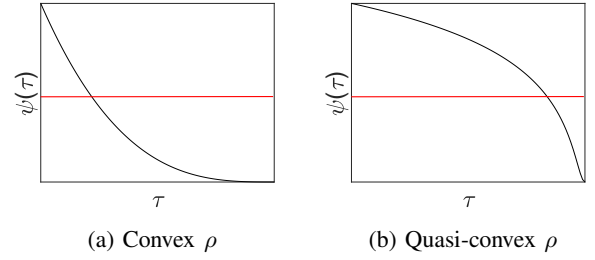


Fig. 1: Pareto frontiers for convex and quasi-convex losses ρ .

TABLE I: Regula Falsi-type methods with different μ values.

Method	μ
Regula Falsi	1
Illinois	0.5
Pegasus	$\frac{f(b)}{f(b)+f(c)}$
Anderson-Björck	$1 - \frac{f(c)}{f(b)}$, and in case $1 \leq \frac{f(c)}{f(b)}$ set $\gamma = 0.5$.

the ρ , bracketing type root finding methods are guaranteed to solve (7). Here, we develop *Regula Falsi* type methods for (7).

We denote the solution of a nonlinear equation of f by x^* , i.e. $f(x^*) = 0$. With this notation, *Regula Falsi* type methods starting with the points a and b proceed as follows.

- 1) Calculate the secant line between a and b ,

$$s_{ab} = \frac{f(b) - f(a)}{b - a}, \quad (8)$$

and find the point where (8) intersects the x -axis, which is $c = b - \frac{f(b)}{s_{ab}}$.

- 2) Calculate $f(c)$. If $f(c) = 0$ then $x^* = c$, otherwise continue.
- 3) Adjust the new interval: if $f(c)f(b) < 0$, x^* should be in between b and c . Set

$$a = b, \quad b = c, \quad \text{and } f(a) = f(b), \quad f(b) = f(c), \quad (9)$$

if $f(c)f(b) > 0$, x^* should be in between a and c .

$$b = c, \quad \text{and } f(a) = \mu f(a), \quad f(b) = f(c), \quad (10)$$

where μ is the scaling factor.

- 4) Check the ending condition: if $|b - a| \leq \epsilon$, stop the iteration. Take

$$x^* = \begin{cases} b, & \text{if } |f(b)| \leq |f(a)| \\ a, & \text{if } |f(b)| > |f(a)| \end{cases}, \quad (11)$$

if $|b - a| > \epsilon$, continue the iteration, go back to 1) with the values a, b and $f(a), f(b)$ from 3).

Regula Falsi type methods differ from each other in the choice of the scaling factor μ . Several commonly considered μ in the literature is summarized in Table I. Additional options for μ are studied in [21], [22].

III. SOLVING (P_σ)

A. (P_τ) Solver

In order to solve (P_σ) , we repeatedly solve (P_τ) . (P_τ) can be solved using the simple projected gradient method

$$\mathbf{x}^{(k)} = \text{proj}_{\tau\mathbb{B}_1} \left(\mathbf{x}^{(k-1)} + \gamma \mathbf{D}^T \nabla \rho(\mathbf{y} - \mathbf{D}\mathbf{x}^{(k-1)}) \right). \quad (12)$$

1) *Projection onto the ℓ_1 -ball*: Projection of a vector $\mathbf{a} = [a_1, a_2, \dots, a_N]$ onto the ℓ_1 -ball can be written as following

$$\text{proj}(\mathbf{a}, \tau) = \begin{cases} \mathbf{a}, & \text{if } \|\mathbf{a}\|_1 \leq 1 \\ \text{sgn}(a_i) \max\{|a_i| - \kappa, 0\}, & \text{else} \end{cases} \quad (13)$$

where κ is the Lagrangian multiplier of $\text{proj}_1(\mathbf{a}, \tau)$ [23]. The tricky part of the projection is to find the κ that satisfies Karush-Kuhn-Tucker optimality condition $\sum_{i=1}^N (|a_i| - \kappa) = \tau$ in an efficient way.

To find κ , we utilized the simple, sorting based approach introduced in [24]. Additional variations of this method are described in [25].

To find κ :

- Sort $|\mathbf{a}|$ as: $c_1 \geq c_2 \geq \dots \geq c_N$,
- Find $K = \max_{1 \leq k \leq N} \left\{ k \mid \left(\sum_{j=1}^k c_j - \tau \right) / k \leq c_k \right\}$,
- Calculate $\kappa = \left(\sum_{k=1}^K c_k - \tau \right) / K$.

To solve (P_τ) , we used a projected gradient method with the spectral line search strategy discussed by [9], with the projection steps given in III-A1.

B. Solving (P_σ)

1) *Bracketing*: In order to choose the root searching interval, we consider a well-known decomposition method called *method of frames (mof)* [26]. The *mof* decomposition of a signal \mathbf{y} can be obtained with the inverse linear mapping such that $\mathbf{x}_{MF} = \mathbf{D}^T (\mathbf{D}\mathbf{D}^T)^{-1} \mathbf{y} = \arg \min \{ \|\mathbf{x}\|_2 \mid \mathbf{y} = \mathbf{D}\mathbf{x} \}$. Many common loss functions ρ are nonnegative and vanish at the origin, including gauges and nonconvex losses considered in this study. For these losses, under the assumption that \mathbf{D} is full row-rank, $\rho(\mathbf{y} - \mathbf{D}\mathbf{x}_{MF}) = 0$ and $\psi(\tau_{MF}) = -\sigma$ with $\tau_{MF} = \|\mathbf{x}_{MF}\|_1$. For the left endpoint, we consider $\mathbf{x} = 0$, and $\tau = 0$, with loss equal to $\rho(\mathbf{y})$. Bracketing the root searching interval between the points \mathbf{x}_{MF} and 0 ensures finding a solution for (7) since they provide two initial points with opposite signs for ψ , as long as $\rho(\mathbf{y}) > \sigma$.

2) *Solving (P_σ)* : We combine the proposed *Regula Falsi* methods and a (P_τ) solver to solve (P_σ) as follows:

- Choose initial τ values.
Choose two initial values with opposite signs to ensure convergence of *Regula Falsi* type Methods. The default choice is given by $\tau = 0$ and $\tau = \tau_{MF}$.
- Apply the steps of *Regula Falsi* type methods.
Every iteration of the *Regula Falsi-type methods* requires solving (P_τ) , except at $\tau = 0$ and $\tau = \tau_{MF}$.
- Terminate once the stopping criteria are met.

IV. SIMULATIONS

In order to examine the performances of *Regula Falsi* type methods given in Table I, we created a test environment and benchmark by using Sparco framework [27]. Real-valued problems are chosen from Sparco for the simulations among this collection of test problems that includes many examples from the literature. Details about the problems and related publications can be found in [27].

Problems	id	M	N	$\rho_l(\mathbf{y})$	$\rho_h(\mathbf{y})$	$\rho_s(\mathbf{y})$
cos-spike	3	1024	2048	102.2423	2378.8	25.09
gauss-en	11	256	1024	99.9055	1272.5	8.957
jitter	902	200	1000	0.4476	4.6881	0.0901

TABLE II: $N, M, \rho(\mathbf{y})$ values for the problem setups.

Performances of the *Regula Falsi* type methods are investigated for three different loss functions ρ which are Least squares $\rho_l(\mathbf{x}) = \|\mathbf{x}\|_2$, Huber

$$\rho_h(\mathbf{x})_i = \sum_{i=1}^N \begin{cases} \frac{x_i^2}{2\delta}, & \text{if } |x_i| \leq \delta \\ |x_i| - \frac{\delta}{2}, & \text{otherwise} \end{cases}, \quad (14)$$

and Student's t $\rho_s(\mathbf{x}) = \sum_{i=1}^N \nu \log(1 + x_i^2/\nu)$ where δ and ν are the tuning parameters for ρ_h and ρ_s , respectively; we take $\delta = 5 \times 10^{-3}$ and $\nu = 10^{-2}$ in our simulations. N, M and $\rho(\mathbf{y})$ values for the chosen problems are given in Table II.

We solve (P_σ) for a range of σ values, chosen relative to $\rho(\mathbf{y})$, in particular $5 \times 10^{-1}\rho(\mathbf{y})$, $5 \times 10^{-2}\rho(\mathbf{y})$ and $5 \times 10^{-3}\rho(\mathbf{y})$. We compute residuals $\rho(\mathbf{r}_\sigma) = \rho(\mathbf{y} - \mathbf{D}\mathbf{x}_\sigma)$, norms $\|\mathbf{x}_\sigma\|_1$, the number of nonzero (*nnz*) for each solution \mathbf{x}_σ , and *iter* the total solves of (P_τ) to reach these solutions; results are displayed in Table III.

Newton's method requires fewer (P_τ) solves (see Table III). However, solving (7) is more expensive for Newton's method than for *Regula Falsi*-type methods since the derivative calculation of the nonlinear equation is required along with the function evaluation, while *Regula Falsi*-type methods need only the function evaluation. From a robustness standpoint, Newton, secant, and their variants are not guaranteed to converge for nonconvex loss functions, in contrast to *Regula Falsi*-type methods.

The Pareto frontier $\nu(\tau)$ is shown for the *gauss-en* problem with losses ρ_l , ρ_h and ρ_s in Figure 2. We expect similar patterns in many problems. As expected, the Pareto frontier is nonconvex, and Newton iterations will not stay in the feasible area for ρ_s in this example, since the tangent lines can leave the feasible region.

Figure 3 shows a typical compressed sensing example. A 20-sparse vector is recovered using a normally distributed Parseval frame $\mathbf{D} \in \mathbb{R}^{175 \times 600}$. A measurement is generated according to $\mathbf{y} = \mathbf{D}\mathbf{x} + \mathbf{w} + \zeta$, where the noise \mathbf{w} is zero mean normal error with the variance of 0.005 and ζ has five randomly placed outliers with a zero mean normal distribution variance of 4. (P_σ) solved with the $\sigma = \rho(\zeta)$ for a fair comparison of ρ_l , ρ_h and ρ_s . Huber loss is less sensitive to outliers in measurement data than least-squares, but Student's t outperforms Huber loss since it grows sublinearly as outliers increase, a property also noted by [11].

V. CONCLUSION

In this note, we developed a new approach using bracketing *Regula Falsi*-type methods, that enable level-set methods to be applied to sparse optimization problems with nonconvex likelihood constraints, significantly expanding their usability. These methods achieve comparable performance to Newton's method for root finding on convex problems, and are guaranteed to converge in the nonconvex case, where Newton and secant variants may fail.

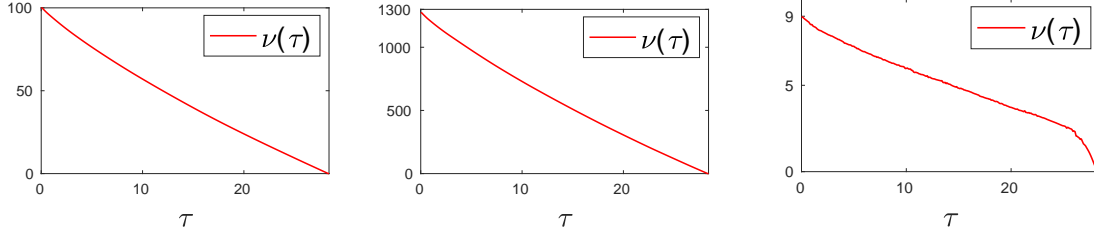


Fig. 2: From left to right, $\nu(\tau)$ for the *gauss-en* problem with ρ_l , ρ_h and ρ_s .

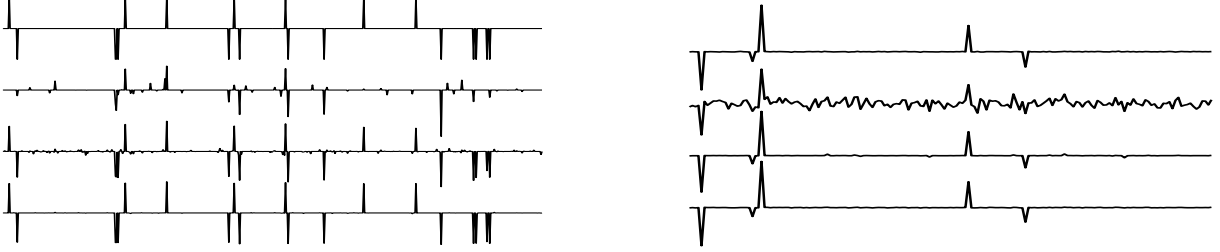


Fig. 3: Left, top to bottom: true signal, reconstructions with *least squares*, *Huber* and *Student's t* losses. Right, top to bottom: true errors, *least squares*, *Huber* and *Student's t* residuals.

TABLE III: Simulation Results for Solving (P_σ).

Problems	$\sigma/\rho(\mathbf{y})$	Methods	<i>least squares</i>				<i>Huber</i> ($\delta = 5 \times 10^{-3}$)				<i>Student's t</i> ($\nu = 10^{-2}$)			
			$\rho_l(\mathbf{r}_\sigma)$	$\ \mathbf{x}_\sigma\ _1$	<i>nnz</i>	<i>iter</i>	$\rho_h(\mathbf{r}_\sigma)$	$\ \mathbf{x}_\sigma\ _1$	<i>nnz</i>	<i>iter</i>	$\rho_s(\mathbf{r}_\sigma)$	$\ \mathbf{x}_\sigma\ _1$	<i>nnz</i>	<i>iter</i>
<i>gauss-en</i>	0.5	Regula Falsi	51.12	66.24	2	10	1189.4	68.328	2	8	12.545	94.289	10	14
		Illinois	51.12	66.24	2	7	1189.4	68.328	2	7	12.545	94.289	10	7
		Pegasus	51.12	66.24	2	7	1189.4	68.328	3	6	12.545	94.289	10	6
		And.-Björck	51.12	66.24	2	9	1189.4	68.328	3	9	12.545	94.289	10	10
		Newton	51.12	66.24	2	3	1189.4	68.328	2	3	—	—	—	—
	0.05	Regula Falsi	5.112	188.4	75	85	118.94	134.71	2	68	1.2105	171.09	79	72
		Illinois	5.112	188.4	75	13	118.94	134.71	2	15	1.2214	172.65	78	16
		Pegasus	5.112	188.4	75	12	118.94	134.71	2	14	1.259	170.95	76	34
		And.-Björck	5.112	188.4	75	27	118.94	134.71	2	32	1.251	170.85	75	50
		Newton	5.112	188.4	75	5	118.94	134.7	2	4	—	—	—	—
	0.005	Regula Falsi	0.511	235.6	123	396	11.893	229.02	127	451	0.1272	231.15	124	383
		Illinois	0.511	235.6	123	19	11.894	229.02	125	15	0.1183	231.15	124	30
		Pegasus	0.511	235.6	123	19	11.894	229.02	130	14	0.118	231.16	121	27
		And.-Björck	0.511	235.6	123	34	11.894	229.02	130	21	0.1273	231.13	122	19
		Newton	0.511	235.6	123	5	11.894	229.02	125	3	—	—	—	—
<i>cos-spike</i>	0.5	Regula Falsi	49.95	11.9	16	9	636.27	11.97	19	9	4.479	16.6	139	11
		Illinois	49.95	11.9	16	7	636.27	11.97	19	6	4.479	16.6	139	8
		Pegasus	49.95	11.9	16	5	636.27	11.97	19	5	4.479	16.6	139	6
		And.-Björck	49.95	11.9	16	7	636.27	11.97	19	7	4.479	16.6	139	8
		Newton	49.95	11.9	16	4	636.27	11.97	19	4	—	—	—	—
	0.05	Regula Falsi	4.995	26.45	35	26	63.63	26.406	50	27	0.448	27.82	39	24
		Illinois	4.995	26.45	35	11	63.63	26.406	50	14	0.448	27.82	39	15
		Pegasus	4.995	26.45	35	11	63.63	26.406	50	11	0.448	27.82	39	15
		And.-Björck	4.995	26.45	35	15	63.63	26.406	50	27	0.448	27.82	39	28
		Newton	4.995	26.45	35	4	63.63	26.406	50	4	—	—	—	—
	0.005	Regula Falsi	0.499	28.06	35	208	6.3624	28.036	46	209	0.045	28.12	1024	207
		Illinois	0.499	28.06	35	19	6.3627	28.036	46	19	0.045	28.12	1024	27
		Pegasus	0.499	28.06	35	19	6.3627	28.036	46	20	0.045	28.12	1024	24
		And.-Björck	0.499	28.06	35	58	6.3627	28.036	46	62	0.045	28.12	1024	65
		Newton	0.499	28.06	35	3	6.3628	28.036	46	4	—	—	—	—
<i>jitter</i>	0.5	Regula Falsi	0.224	0.766	3	7	2.344	0.6959	3	7	0.045	0.4548	2	9
		Illinois	0.224	0.766	3	6	2.344	0.6958	3	7	0.045	0.4548	2	7
		Pegasus	0.224	0.766	3	6	2.344	0.6958	3	6	0.045	0.4548	2	6
		And.-Björck	0.224	0.766	3	8	2.344	0.6958	3	8	0.045	0.4548	2	9
		Newton	0.224	0.766	3	3	2.344	0.6958	3	3	—	—	—	—
	0.05	Regula Falsi	0.022	1.537	3	39	0.2343	1.4338	3	43	0.005	1.2587	3	54
		Illinois	0.022	1.537	3	12	0.2344	1.4338	3	15	0.005	1.2585	3	14
		Pegasus	0.022	1.537	3	12	0.2344	1.4338	3	14	0.005	1.2585	3	12
		And.-Björck	0.022	1.537	3	30	0.2344	1.4338	3	39	0.005	1.2585	3	41
		Newton	0.022	1.537	3	2	0.2344	1.4338	3	4	—	—	—	—
	0.005	Regula Falsi	0.002	1.614	3	375	0.0233	1.5646	3	391	0.0005	1.5086	3	413
		Illinois	0.002	1.614	3	19	0.0234	1.5644	3	16	0.0005	1.508	3	16
		Pegasus	0.002	1.614	3	20	0.0234	1.5644	3	14	0.0005	1.508	3	16
		And.-Björck	0.002	1.614	3	35	0.0234	1.5644	3	27	0.0005	1.508	3	107
		Newton	0.002	1.614	3	2	0.0235	1.5643	3	5	—	—	—	—

REFERENCES

- [1] E. J. Candes, J. Romberg, and T. Tao, "Robust uncertainty principles: exact signal reconstruction from highly incomplete frequency information," *IEEE Transactions on Information Theory*, vol. 52, no. 2, pp. 489–509, 2006.
- [2] D. L. Donoho, "Compressed sensing," *IEEE Trans. Inf. Theor.*, vol. 52, no. 4, p. 1289–1306, Apr. 2006. [Online]. Available: <https://doi.org/10.1109/TIT.2006.871582>
- [3] D. L. Donoho and X. Huo, "Uncertainty principles and ideal atomic decomposition," *IEEE Transactions on Information Theory*, vol. 47, no. 7, pp. 2845–2862, 2001.
- [4] J. . Fuchs, "On sparse representations in arbitrary redundant bases," *IEEE Transactions on Information Theory*, vol. 50, no. 6, pp. 1341–1344, 2004.
- [5] E. J. Candes and T. Tao, "Decoding by linear programming," *IEEE Transactions on Information Theory*, vol. 51, no. 12, pp. 4203–4215, 2005.
- [6] M. Lustig, J. H. Lee, D. L. Donoho, and J. M. Pauly, "Faster imaging with randomly perturbed, undersampled spirals and $—|—|$ reconstruction," in *Proceedings of the 13th Annual Meeting of ISMRM*, 2005, p. 685.
- [7] A. Y. Aravkin, J. V. Burke, D. Drusvyatskiy, M. P. Friedlander, and S. Roy, "Level-set methods for convex optimization," *Mathematical Programming*, vol. 174, no. 1, pp. 359–390, 2019.
- [8] S. Foucart and H. Rauhut, *A Mathematical Introduction to Compressive Sensing*, ser. Applied and Numerical Harmonic Analysis. Springer New York, 2013.
- [9] E. van den Berg and M. Friedlander, "Probing the pareto frontier for basis pursuit solutions," *SIAM Journal on Scientific Computing*, vol. 31, no. 2, pp. 890–912, 2009. [Online]. Available: <https://doi.org/10.1137/080714488>
- [10] —, "Sparse optimization with least-squares constraints," *SIAM Journal on Optimization*, vol. 21, no. 4, pp. 1201–1229, 2011. [Online]. Available: <https://doi.org/10.1137/100785028>
- [11] A. Y. Aravkin, J. V. Burke, and M. P. Friedlander, "Variational properties of value functions," *SIAM Journal on optimization*, vol. 23, no. 3, pp. 1689–1717, 2013.
- [12] G. Dahlquist and Å. Björck, *Numerical Methods*, ser. Dover Books on Mathematics. Dover Publications, 2003. [Online]. Available: <https://books.google.de/books?id=armfeHpJlwAC>
- [13] N. Städler, P. Buehlmann, and S. Van De Geer, " l_1 -penalization for mixture regression models," *Test*, vol. 19, no. 2, pp. 209–256, 2010.
- [14] P. Buehlmann and S. Geer, "Non-convex loss functions and l_1 -regularization," *Statistics for High-Dimensional Data*, pp. 293–338, 2011.
- [15] "Robust and trend-following kalman smoothers using student's t^* ," *IFAC Proceedings Volumes*, vol. 45, no. 16, pp. 1215 – 1220, 2012, 16th IFAC Symposium on System Identification.
- [16] A. Y. Aravkin, J. V. Burke, and G. Pillonetto, "Sparse/robust estimation and kalman smoothing with nonsmooth log-concave densities: Modeling, computation, and theory," *The Journal of Machine Learning Research*, vol. 14, no. 1, pp. 2689–2728, 2013.
- [17] A. Aravkin, M. P. Friedlander, F. J. Herrmann, and T. Van Leeuwen, "Robust inversion, dimensionality reduction, and randomized sampling," *Mathematical Programming*, vol. 134, no. 1, pp. 101–125, 2012.
- [18] P. M. Pardalos, A. Žilinskas, and J. Žilinskas, *Non-convex multi-objective optimization*. Springer, 2017.
- [19] K. Miettinen, "Some methods for nonlinear multi-objective optimization," in *International conference on evolutionary multi-criterion optimization*. Springer, 2001, pp. 1–20.
- [20] E. Van den Berg, "Convex optimization for generalized sparse recovery," Ph.D. dissertation, University of British Columbia, 2009.
- [21] S. Galdino, "A family of regula falsi root-finding methods."
- [22] J. A. Ford, "Improved algorithms of illinois-type for the numerical solution of nonlinear equations."
- [23] J. Duchi, S. Shalev-Shwartz, Y. Singer, and T. Chandra, "Efficient projections onto the l_1 -ball for learning in high dimensions," in *ICML '08: Proceedings of the 25th international conference on Machine learning*, New York, NY, USA, 2008, pp. 272–279. [Online]. Available: <http://doi.acm.org/10.1145/1390156.1390191>
- [24] M. Held, P. Wolfe, and H. P. Crowder, "Validation of subgradient optimization," *Math. Program.*, vol. 6, no. 1, pp. 62–88, Dec. 1974. [Online]. Available: <https://doi.org/10.1007/BF01580223>
- [25] L. Condat, "Fast Projection onto the Simplex and the l_1 Ball," *Mathematical Programming, Series A*, vol. 158, no. 1, pp. 575–585, Jul. 2016. [Online]. Available: <https://hal.archives-ouvertes.fr/hal-01056171>
- [26] I. Daubechies, "Time-frequency localization operators: a geometric phase space approach," *IEEE Transactions on Information Theory*, vol. 34, no. 4, pp. 605–612, July 1988.
- [27] E. van den Berg, M. P. Friedlander, G. Hennenfent, F. J. Herrmann, R. Saab, and O. Yilmaz, "Algorithm 890: Sparco: A testing framework for sparse reconstruction," *ACM Trans. Math. Softw.*, vol. 35, no. 4, Feb. 2009. [Online]. Available: <https://doi.org/10.1145/1462173.1462178>